Received: *August 14, 1998,* Accepted: *December 16, 1998*

Oscillations of solar and atmospheric neutrinos*

Riccardo Barbieri
Scuola Normale Superiore, and INFN, sezione di Pisa, I-56126 Pisa, Italy
E-mail: barbieri@difi.unipi.it

Lawrence J. Hall, David Smith and Neil J. Weiner
Department of Physics and
Theoretical Physics Group, Lawrence Berkeley National Laboratory
University of California, Berkeley, California 94720
E-mail: LJHall@lbl.gov, drsmith@thsrv.lbl.gov, NJWeiner@lbl.gov

Alessandro Strumia
Dipartimento di fisica, Università di Pisa, and INFN, sezione di Pisa,
I-56127 Pisa, Italia
E-mail: astrumia@difi.unipi.it

Abstract: Motivated by recent results from SuperKamiokande, we study both solar and atmospheric neutrino fluxes in the context of oscillations of the three known neutrinos. We aim at a global view which identifies the various possibilities, rather than attempting the most accurate determination of the parameters of each scenario. For solar neutrinos we emphasise the importance of performing a general analysis, independent of any particular solar model and we consider the possibility that any one of the techniques — chlorine, gallium or water Cerenkov — has a large unknown systematic error, so that its results should be discarded. The atmospheric neutrino anomaly is studied by paying special attention to the ratios of upward and downward going ν_e and ν_μ fluxes. Both anomalies can be described in a minimal scheme where the respective oscillation frequencies are widely separated or in non-minimal schemes with two comparable oscillation frequencies. We discuss explicit forms of neutrino mass matrices in which both atmospheric and solar neutrino fluxes are explained. In the minimal scheme we identify only two 'zeroth order' textures that can result from unbroken symmetries. Finally we discuss experimental strategies for the determination of the various oscillation parameters.

Keywords: Solar and Atmospheric Neutrinos, Beyond Standard Model, Neutrino Physics.

JHEP12(1998)017

Contents

1. Introduction **1**

2. Solar neutrinos: model-independent analysis **3**
2.1 Model-independent solar analysis — all experiments 6
2.2 Model independent solar analysis — one experiment ignored 10

3. Atmospheric and solar neutrinos: the minimal scheme **12**

4. Atmospheric and solar neutrinos: non-minimal schemes **15**

5. Large $\nu_\mu \to \nu_\tau$ mixing for atmospheric neutrinos **18**
5.1 2×2 matrix forms 18
5.2 3×3 matrix forms 20

6. Models for both solar and atmospheric neutrinos **20**
6.1 $L_e - L_\mu - L_\tau$ realized in the low energy effective theory 22
6.2 $L_e - L_\mu - L_\tau$ realized via the seesaw mechanism 23

7. Conclusions **25**

1. Introduction

The solar and atmospheric neutrino flux anomalies have both been considerably strengthened by recent observations from Super-Kamiokande. The solar neutrino flux is measured to be [1] 0.37 ± 0.03 of that expected from the 'BP95' standard solar model [2], without including any theoretical error. This is the fifth solar neutrino experiment to report results in strong disagreement with the predictions of solar models. Furthermore, using a solar model independent analysis, the measured solar fluxes are found to be in conflict with each other. For events at SuperKamiokande with visible energies of order a GeV, the ratio of 1 ring μ-like to e-like events is 0.66 ± 0.10 that expected from calculations of the flux of neutrinos produced in the atmosphere in cosmic ray showers [3]. Furthermore, the distribution in zenith angle

*This work was supported in part by the U.S. Department of Energy under Contracts DE-AC03-76SF00098, in part by the National Science Foundation under grant PHY-95-14797, in part by the TMR network under the EEC contract n. ERBFMRX-CT960090.

of these 1 ring events provides striking evidence for a depletion of ν_μ which depends on the distance travelled by the neutrinos before reaching the Super-Kamiokande detector. In particular, the observed up/down ratio of the multi-GeV, μ-like events is 0.52 ± 0.07. This significantly strengthens the evidence that ν_μ oscillate as they traverse the earth.

In this paper, we interpret the solar and atmospheric neutrino flux anomalies in terms of oscillations of the three known neutrinos $\nu_{e,\mu,\tau}$. The lightness of these three neutrinos, relative to the charged fermions, can be simply understood as resulting from large $\mathrm{SU}(2)_L \otimes \mathrm{U}(1)_Y$ invariant masses for the right-handed neutrinos, via the see-saw mechanism. We do not consider the possibility of a fourth light neutrino, as it would have to be singlet under $\mathrm{SU}(2)_L \otimes \mathrm{U}(1)_Y$, and would either require a new mass scale far below the weak scale, running counter to the idea of the see-saw mechanism, or a more complicated see-saw.

Theoretical ideas about generation mixing are guided by the quark sector, where the mixing angles are all small, indicating a hierarchical breaking of horizontal symmetries in nature. A similar hierarchy of horizontal symmetry breaking in the lepton sector is also likely to yield small angles, suggesting small probabilities for a neutrino to oscillate from one flavour to another. However, the solar and atmospheric neutrino flux measurements both require neutrino survival probabilities, P_{ee} and $P_{\mu\mu}$, far from unity. Over a decade ago [4], it was realised that large angles were not necessary to account for the large suppression of solar neutrino fluxes — while ν_e have charged current interactions in the solar medium, $\nu_{\mu,\tau}$ do not, allowing a level crossing phenomena where a ν_e state produced in the solar interior evolves to a $\nu_{\mu,\tau}$ state as it traverses the sun. This simple picture can reconcile the three types of solar neutrino flux measurements with the standard solar model, for a mixing angle as small as 0.03 — a significant achievement. Could such resonant oscillations occur for atmospheric neutrinos in the earth, again allowing a small vacuum mixing angle? In this case, since the earth does not have a continuously varying density, the matter mixing angle in the earth is much larger than the vacuum mixing angle only in a small range of energies. Hence, an oscillation interpretation of the atmospheric neutrino fluxes requires a large mixing angle, and calls into question the frequently stated theoretical prejudice in favour of small mixing angles.

In this paper, we attempt to understand both solar and atmospheric neutrino fluxes using 3-generation neutrino oscillations, aiming at a global view which identifies the various possibilities, rather than attempting the most accurate determination of the parameters of each scenario. When data from chlorine, gallium and water Cerenkov detectors are fitted to a standard solar model, standard analyses find very small regions of neutrino mass and mixing parameters. For 2-generation mixing, these are known as the “small angle MSW”, “large angle MSW” and “just so” regions. This analysis has been extended to the case of three generations [5], with a single matter resonance in the sun, as suggested by the atmospheric neutrino data.

The large and small angle MSW areas are found to merge into a single MSW volume of parameter space. In subsection 2.1, we study how this volume is enlarged when a solar model independent analysis of the solar fluxes replaces the use of a single solar model. In subsection 2.2 we extend our analysis to see what areas of neutrino parameter space become allowed if one of the three observational techniques to measure the solar fluxes is seriously in error.

We combine these regions of parameters with those yielding the atmospheric fluxes, and find there is still considerable allowed ranges of masses and mixing angles. This is done in section 3, assuming that the smallest of the two neutrino squared mass differences is too small to affect the oscillations of atmospheric neutrinos (minimal scheme). In section 4, on the contrary, we allow for the possibility that the two independent neutrino squared mass differences are both large enough to affect atmospheric neutrino oscillations (non minimal schemes). For solar neutrinos, this requires that there is a serious flaw either in at least one measurement technique or in solar model analyses.

The forms of neutrino mass matrices that can lead to a large $\nu_\mu \rightleftharpoons \nu_\tau$ mixing for atmospheric neutrinos are discussed in section 5. In section 6 only two 'zeroth order' textures for neutrinos masses are identified that can account for the atmospheric and solar neutrino data in the minimal scheme and can result from unbroken symmetries.

Our conclusions are drawn in section 7. Based on a simple set of alternative hypotheses, we discuss how future measurements could eventually determine the two neutrino mass differences and the three mixing angles.

2. Solar neutrinos: model-independent analysis

In the flavour eigenstate basis, in which the charged lepton mass matrix is diagonal, the neutrino mass matrix is in general non-diagonal. It may be diagonalized by a unitary transformation:

$$\nu_f = V^*_{fi}\nu_i\,, \tag{2.1}$$

where ν_f and ν_i are flavour and mass eigenstate fields, respectively. The leptonic analogue of the Cabibbo-Kobayashi-Maskawa mixing matrix is V^T, since the W boson couples to the charged current $\bar{\nu}_{i_L} V^T_{if}\gamma^\mu e_{f_L}$. In addition to the three Euler angles, V contains physical phases: one if the light neutrinos are Dirac, and three if they are Majorana. These flavour and mass eigenstate fields destroy basis states which are related by

$$|\nu_f\rangle = V_{fi}|\nu_i\rangle\,. \tag{2.2}$$

If some process creates a flavour eigenstate, $|\nu_f\rangle$, at time $t=0$, then at a later time t it will have evolved to the state $|\nu_f, t\rangle = \psi_{f'}(t)|\nu_{f'}\rangle$ via the matrix Schroedinger

JHEP12(1998)017

equation

$$i\frac{d\psi}{dt} = \left(V\frac{m_\nu^2}{2E}V^\dagger + A_{\rm CC} + \mathcal{E} \right)\psi\,, \tag{2.3}$$

where E is the energy of the relativistic neutrino, m_ν is the diagonal neutrino mass matrix with entries m_i, $\mathcal{E}$ is an irrelevant term proportional to the unit matrix, and $A_{\rm CC}$ represents matter effects. For neutrinos propagating in matter with electron number density N_e, $A_{\rm CC}$ is a matrix with a single non-zero entry, $A_{\rm CC}^{11} = \sqrt{2}G_F N_e$.

The mixing matrix V can be written quite generally as

$$V = R_{23}(\theta_{23})\begin{pmatrix} 1 & 0 & 0 \\ 0 & e^{i\phi} & 0 \\ 0 & 0 & 1 \end{pmatrix} R_{13}(\theta_{13})R_{12}(\theta_{12})\begin{pmatrix} 1 & 0 & 0 \\ 0 & e^{i\alpha} & 0 \\ 0 & 0 & e^{i\beta} \end{pmatrix}, \tag{2.4}$$

where $R_{ij}(\theta_{ij})$ represents a rotation by θ_{ij} in the ij plane. We have chosen a sequence of rotations which frequently arises in the diagonalization of simple hierarchical forms for the neutrino mass matrix, as illustrated in section 6. From equation (2.3) we see that the phases α and β never appear in oscillation phenomena, and hence can be dropped, giving

$$V = \begin{pmatrix} c_{12}c_{13} & c_{13}s_{12} & s_{13} \\ -c_{23}s_{12}e^{i\phi} - c_{12}s_{13}s_{23} & c_{12}c_{23}e^{i\phi} - s_{12}s_{13}s_{23} & c_{13}s_{23} \\ s_{23}s_{12}e^{i\phi} - c_{12}c_{23}s_{13} & -c_{12}s_{23}e^{i\phi} - c_{23}s_{12}s_{13} & c_{13}c_{23} \end{pmatrix}. \tag{2.5}$$

Each R_{ij} must diagonalize a symmetric 2×2 sub-matrix determining $\tan 2\theta_{ij}$, hence, without loss of generality, we may choose $0 \le \theta_{ij} \le \pi/2$, while $0 \le \phi < 2\pi$. A more convenient choice is to keep $\theta_{12,13}$ in the first quadrant, while $0 \le \theta_{23}, \phi \le \pi$. We choose to order the neutrino mass eigenstates so that $\Delta m^2_{23} > \Delta m^2_{12} > 0$, where $\Delta m^2_{ij} \equiv m_i^2 - m_j^2$. Notice that with this parametrization $V_{e3} \ll 1$ means θ_{13} close to 0 or to 90°.

To study solar neutrinos, we are interested only in the electron neutrino survival probability, P_{ee}, and hence in the evolution of ψ_e. This evolution does not depend on θ_{23} or on ϕ — on substituting (2.4) in (2.3), R_{23} and ϕ can be absorbed into redefined states μ' and τ'. Hence, we have shown quite generally that P_{ee} depends only on four neutrino parameters: Δm^2_{12}, Δm^2_{23}, θ_{12} and θ_{13}.

For an oscillation explanation of the atmospheric neutrino fluxes, Δm^2_{23} is sufficiently large that it does not cause a resonance transition in the sun. In the Landau-Zehner approximation, the evolution equation (2.3) can be solved to give [6]

$$P_{ee} = \left(|V_{e1}|^2, |V_{e2}|^2, |V_{e3}|^2\right)\begin{pmatrix} 1-P & P & 0 \\ P & 1-P & 0 \\ 0 & 0 & 1 \end{pmatrix}\begin{pmatrix} |V^{\rm m}_{e1}|^2 \\ |V^{\rm m}_{e2}|^2 \\ |V^{\rm m}_{e3}|^2 \end{pmatrix} \tag{2.6}$$

where $V^{\rm m}_{ei}$ are the mixing matrix elements in matter, and P is the transition probability between the states at resonance:

$$\begin{aligned} P &= e^{-E_{\rm NA}/E}\theta(E-E_{\rm A})\,, \\ E_{\rm NA} &= \frac{\pi\Delta m_{12}^2\sin^2(2\theta_{12})}{4|\frac{1}{N_e}\frac{dN_e}{dx}|_1\cos(2\theta_{12})}\,, \\ E_{\rm A} &= \frac{\Delta m_{12}^2\cos 2\theta_{12}}{2\sqrt{2}G_{\rm F}|N_e|_0\cos^2\theta_{13}}\,. \end{aligned} \tag{2.7}$$

Here E is the neutrino energy, θ is the step function, the 1 subscript indicates that N_e and its gradient dN_e/dx are evaluated at the resonance point, while the 0 subscript indicates the production point. The large mass splitting Δm_{23}^2 enters P_{ee} only via the matter mixing angles, and decouples from these expressions in the limit that it is much larger than $A_{11}E$, and also in the limit that θ_{13} vanishes. For most of this section we make Δm_{23}^2 sufficiently large that it decouples, and we comment at the end on the effect on the allowed regions of parameter space for non-zero θ_{13} and small Δm_{23}^2, where Δm_{23}^2 effects may not decouple.

The signals S_i at the three types of solar neutrino experiments are

$$S_i = \int dE\,\Phi(E)\left[\sigma_i^e(E)P_{ee}(E) + \sigma_i^{\not e}(E)\Big(1-P_{ee}(E)\Big)\right], \qquad i = \{\mathrm{SK}, \mathrm{Ga}, \mathrm{Cl}\}\,, \tag{2.8}$$

where $\Phi(E)$ is the total flux of solar neutrinos with energy E, and $\sigma_i^{e,\not e}(E)$ are the interaction cross sections at experiment i for electron-type and non-electron-type neutrinos, respectively (only the water Cerenkov detectors are sensitive to neutral currents, so $\sigma_{\rm Ga}^{\not e}(E) = \sigma_{\rm Cl}^{\not e}(E) = 0$). We will use the theoretical predictions of the various cross sections found in [7, 8]. The flux $\Phi(E)$ is broken into components in the standard way by specifying the production reaction, giving [7]

$$\Phi(E) = \sum_\alpha \Phi_\alpha f_\alpha(E)\,, \qquad \text{with} \qquad \int_0^\infty f_\alpha(E)\,dE = 1 \tag{2.9}$$

and $\alpha = \mathrm{pp}, \mathrm{pep}, {}^7\mathrm{Be}, {}^{13}\mathrm{N}, {}^{15}\mathrm{O}, {}^{17}\mathrm{F}, {}^8\mathrm{B}, h\mathrm{ep}$. At this point we follow the (nearly) model-independent treatment of the fluxes described in [9] by making the following assumptions:

1. The energy dependence $f_\alpha(E)$ of the single components of the neutrino fluxes predicted by solar models ([7, 2] for instance) are correct. In fact the $f_\alpha(E)$ do not depend on the structure of the sun, and are the same in any solar model that does not introduce non-standard electroweak effects [7].

2. The overall Φ_α can differ from their solar models predictions. However there are strong physical reasons to believe that the ratios $\Phi_{^{13}\mathrm{N}}/\Phi_{^{15}\mathrm{O}}$ and $\Phi_{\rm pep}/\Phi_{\rm pp}$ can be set to their solar SM values [2]. Furthermore we neglect entirely hep and ^{17}F neutrinos, which we expect to be extremely rare.

3. The present total luminosity of the sun, $K_\odot$, determines its present total neutrino luminosity as

$$K_\odot = \sum_\alpha \left(\frac{Q}{2} - \langle E_{\nu_\alpha}\rangle\right)\Phi_\alpha \approx \frac{Q}{2}\sum_\alpha \Phi_\alpha\,, \tag{2.10}$$

where $Q = 26.73$ MeV is the energy released in the reaction $4\mathrm{p}+2e \to {}^4\mathrm{He}+2\nu_e$, and $K_\odot = 8.53\cdot 10^{11}$ MeV cm^{-2} s^{-1} is the solar radiative flux at the earth. Using (2.10) amounts to assuming that the solar energy comes from nuclear reactions that reach completion, and that the sun is essentially static over the 10^4 years employed by photons to random-walk out of the solar interior.

After the first assumption we have one free parameter Φ_α for each α; the second then reduces the number of free parameters to four, which we can take to be

$$\begin{aligned}
&\Phi_{\rm p} \equiv \Phi_{\rm pp} + \Phi_{pep}\,,\\
&\Phi_{\rm CNO} \equiv \Phi_{^{13}\rm N} + \Phi_{^{15}\rm O}\,,\\
&\Phi_{^7\rm Be}\,,\\
&\Phi_{^8\rm B}\,.
\end{aligned} \tag{2.11}$$

The luminosity constraint allows us to eliminate $\Phi_{\rm p}$, giving

$$S_i = S_i\left(\Delta m^2_{12},\,\theta_{12},\,\theta_{13};\Phi_{^8\rm B},\Phi_{^7\rm Be},\frac{\Phi_{\rm CNO}}{\Phi_{^7\rm Be}}\right). \tag{2.12}$$

Since solar models give a stable prediction for $\Phi_{\rm CNO}/\Phi_{^8\rm B} = 0.22$ [9], we have singled out this ratio and we will use its SSM value in our analysis. Variations of even an order of magnitude in the ratio affect negligibly our final results, since the two neutrino components have similar cross sections in existing detectors.

2.1 Model-independent solar analysis — all experiments

The signals now depend only on $\Phi_{^8\rm B}$ and $\Phi_{^7\rm Be}$, so that, for any given oscillation pattern $P_{ee}(E)$ it is possible to plot the three experimental results[1] [1, 10, 11, 12]

$$S^{\rm exp}_{\rm Cl} = (2.54\pm 0.20)\ 10^{-36}{\rm s}^{-1}\,, \tag{2.13}$$
$$S^{\rm exp}_{\rm Ga} = (75\pm 7)\ 10^{-36}{\rm s}^{-1} \tag{2.14}$$
$$S^{\rm exp}_{\rm SK} = (2.51\pm 0.16)\cdot 10^{6}\,{\rm cm}^{-2}{\rm s}^{-1}\,, \tag{2.15}$$

as three bands in the ($\Phi_{^8\rm B}$, $\Phi_{^7\rm Be}$) plane. The three bands will in general not meet, giving interesting solar model independent restrictions on the oscillations parameters.

[1]The SuperKamiokande experimentalists give directly the value of the flux they measure. The other experiments involve more uncertain neutrino cross sections and prefer to give the frequency of events measured per target atom in their detector. For simplicity we have omitted this detail in the text, leaving a trivial inconsistency between eq. (2.15) and (2.8).

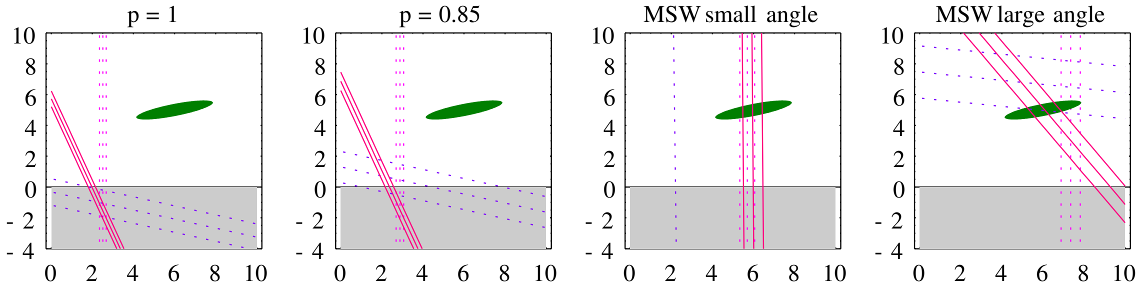

Figure 1: Values of $(\Phi_{^8\mathrm{B}}, \Phi_{^7\mathrm{Be}})$ measured by the Chlorine experiment (continuous lines), the Gallium experiment (dashed lines) and by the SuperKamiokande experiment (long dashed lines) assuming various neutrino oscillation schemes: • no oscillation in fig. 1a; • an energy-independent $P(\nu_e \to \nu_e) = 0.85$ in fig. 1b; • the best-fit point of the small-angle MSW oscillation in fig. 1c; • the best-fit point of the large-angle MSW oscillation in fig. 1d.

We begin the analysis studying the case of *no neutrino oscillations* ($P_{ee} = 1$). In this particular case the solar model independent analysis does not give a strong result. Surprisingly the three bands perfectly meet [9, 13] as shown in fig. 1a, but mainly in the unphysical $\Phi_{^7\mathrm{Be}} < 0$ region, with a small area in the physical region lying within 2σ of each central value. Since the physical crossing region has a negligible ^{7}Be flux, the value of $\Phi_{\mathrm{CNO}}/\Phi_{^7\mathrm{Be}}$ becomes completely irrelevant.

To discuss this case in a quantitative way and to deal with more general cases it is useful to introduce the χ-square function

$$\chi^2_\lambda\left(P_{ee}(\Delta m^2_{12}, \theta_{12}, \theta_{13}), \Phi_{^8\mathrm{B}}, \Phi_{^7\mathrm{Be}}\right) \equiv \sum_i \left(\frac{S_i - S_i^{\mathrm{exp}}}{\Delta S_i^{\mathrm{exp}}}\right)^2 + \sum_{jk} \frac{\left(\Phi_j - \Phi_j^{\mathrm{SSM}}\right)\left(\Phi_k - \Phi_k^{\mathrm{SSM}}\right)}{\lambda^2 \Delta\Phi^{2\,\mathrm{SSM}}_{jk}} \tag{2.16}$$

where $\Delta S_i^{\mathrm{exp}}$ is the 1σ uncertainty for experiment i, given in (2.13)–(2.15), Φ^{SSM} is the flux prediction of the solar model [2] and $\Delta\Phi^{\mathrm{SSM}}$ is the corresponding error matrix, taken with some generosity. The 1σ ranges of $\Phi_{^8\mathrm{B}}$ and $\Phi_{^7\mathrm{Be}}$ are represented by the ellipse in fig. 1. We perform our analysis with two choices for $\Delta\Phi = \lambda \cdot \Delta\Phi^{\mathrm{SSM}}$. We call the first choice, $\Delta\Phi = \Delta\Phi^{\mathrm{SSM}}$, "*solar SM inspired*"). The second choice, $\Delta\Phi = 8 \cdot \Delta\Phi^{\mathrm{SSM}}$ ("*model independent*") has the same shape as the first, but is eight times as large. The part of the analysis done using this $\Delta\Phi$ is virtually free of solar physics input. The choice $\lambda = 8$ (rather than $\lambda = \infty$) avoids unnatural values of $\Phi_{^7\mathrm{Be}}$. This choice essentially ignores solar physics considerations, but the virtue of having a number of independent experimental results is precisely that we need no longer rely heavily on solar modelling to gain insight into the underlying particle physics.

Minimizing the χ^2 in the positive flux region we obtain $\min \chi^2_8(P_{ee} = 1) = 8.25$.

JHEP12(1998)017

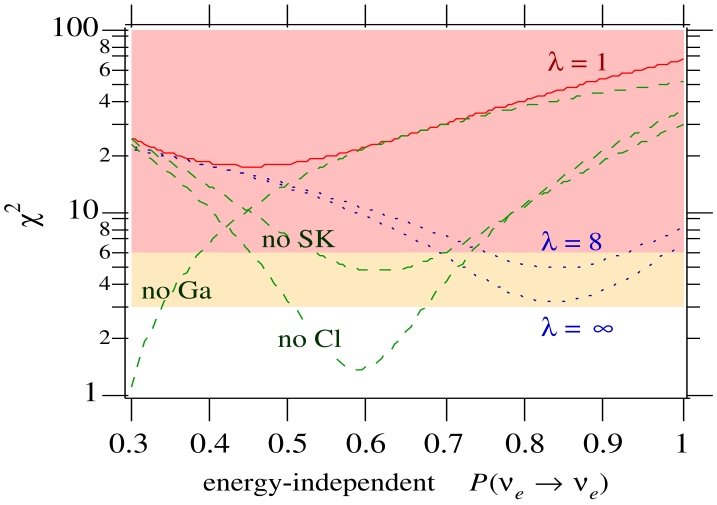

Figure 2: Values of the χ-square as function of an energy independent $P(\nu_e \to \nu_e)$. The parameter λ is defined in eq. (2.17). Also shown is the χ^2 with one experiment discarded and $\lambda = 1$.

The usual criterion for goodness of fit says that a χ^2 with one degree of freedom larger than 8.25 is obtained with a very small probability, $\wp \approx 0.4\%$ (a careful Monte Carlo treatment of the $\Phi_{^7\mathrm{Be}} > 0$ constraint gives similar results [13]). We however remark that, if the sun really emits the best-fit fluxes, $\Phi_{^7\mathrm{Be}} = 0$ and $\Phi_{^8\mathrm{B}} = 2.5\ 10^6/\mathrm{cm}^2\mathrm{s}$, there is a 10% probability that statistical fluctuations produce the present experimental data.

We can just as easily investigate the slightly more general case of an energy independent P_{ee}.The dependence on the neutrino parameters Δm^2_{12}, θ_{12}, and θ_{13} arises through P_{ee}; if the survival probability is a constant, then we can minimize χ^2_λ in the positive-flux region, for any value of P_{ee}, to obtain $\min\chi^2_\lambda(P_{ee})$, which is plotted in fig. 2 for $\lambda = 1$ (SSM analysis), $\lambda = 8$ (SSM independent analysis) and $\lambda = \infty$ (completely model independent analysis). For $P_{ee} \sim 0.85$, $\min\chi^2_8$ drops to 5, but the fluxes required to get relatively small χ^2 values are disfavoured by solar physics considerations — Φ_{CNO} and $\Phi_{^7\mathrm{Be}}$ must be nearly made to vanish, as shown in fig 1b. When $P_{ee} \lesssim 1/2$ the (accidental?) threefold crossing no longer occurs, so that this case can be firmly excluded in a solar-model independent way [9, 14] (see fig. 2). However, as we shall see in subsection 2.2, once we allow for the possibility that one type of experiment's results should be discarded, it is possible to obtain good fits of the data for constant $P_{ee} \sim 1/2$ without having to resort to unnatural flux values.

Of course, we are interested in any points in parameter space that fit the data well, regardless of whether they lead to constant P_{ee}. For any values of Δm^2_{12}, θ_{12}, and θ_{13} we can make plots similar to fig. 1a.

Figs. 1c and 1d show two examples that illustrate the familiar 2-generation small and large angle MSW solutions, which evidently fit the data well if standard solar model fluxes are used.

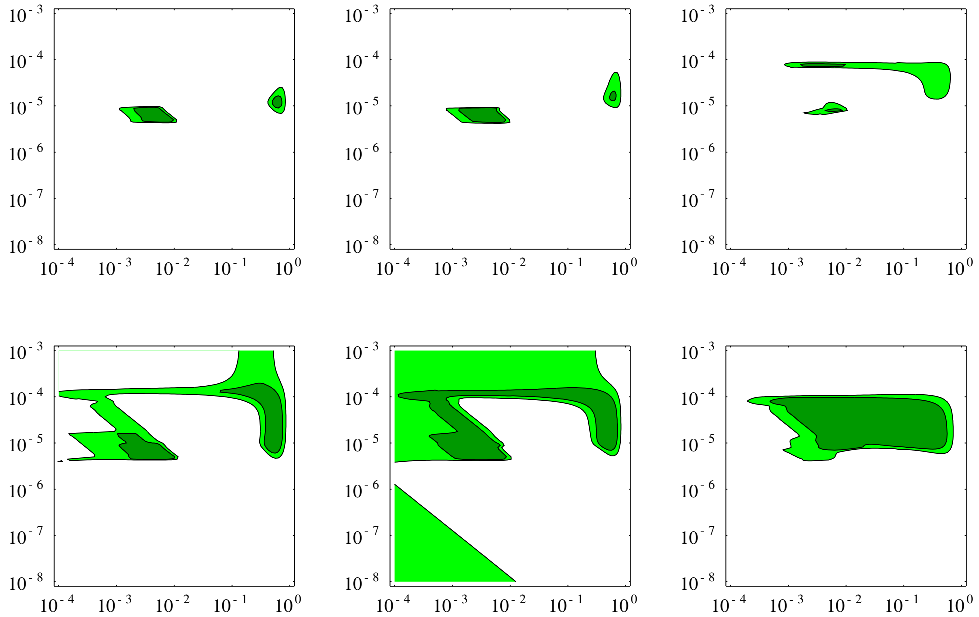

Figure 3: Allowed regions in the plane $(\sin^2 2\theta_{12}, \Delta m^2_{12})$ for $\theta_{13} = 0, 15^\circ$ and 30°. The upper plots assume that the BP solar model is correct. The lower plots are the result of the solar model independent analysis described in the text.

In fig. 3 we show how the allowed regions in neutrino parameter space change if we let the fluxes vary over an expanded range of values. For each point in (Δm^2_{12}, θ_{12}, θ_{13}) space, we minimize χ^2_1 and χ^2_8 by varying the fluxes within the physical region, and then we plot contours of $\min \chi^2_\lambda$ in the ($\sin^2(2\theta_{12})$, Δm^2_{12}) plane for various values of θ_{13}. The results for the "SSM inspired" and "model independent" analyses are shown in figs. 3 (upper row and lower row, respectively). The contours are for $\chi^2 = 3$ and $\chi^2 = 6$.

For small θ_{13} the "*SSM inspired*" results show the standard small and large angle MSW regions. For larger values of θ_{13}, the two MSW regions join, and, as θ_{13} approaches $\pi/4$, the solutions with large θ_{12} disappear. For $\theta_{13} = \pi/4$ the region with $\min \chi^2_1 < 3$ is in fact absent entirely.

The "*model independent*" results similarly exhibit a very strong θ_{13} dependence. We see that the "model independent" analysis continues to give strong restrictions of the oscillation parameters — in particular the Δm^2_{12} values with $\min \chi^2_8 < 3$ are always in the range $\sim 10^{-(4\div 5)}\,\mathrm{eV}^2$. This will not remain true when we consider the consequences of ignoring one experiment's data in subsection 2.2.

If $\Phi_{\rm CNO}/\Phi_{^8\rm B}$ is ten times larger than in SSM there are new allowed regions. However these possible new regions, with $\Delta m^2 = 10^{-(5\div 6)}\,\mathrm{eV}^2$ and $\sin^2 2\theta_{12} \gtrsim 10^{-2}$, are excluded in a model-independent way by the non observation of a day/night asym-

JHEP12(1998)017

metry at SuperKamiokande [1, 15]. The recent data [1] on this asymmetry in fact disfavour as well the large angle MSW solution of the SSM-inspired analysis. Moreover, we have not included in our χ^2 analysis the SuperKamiokande measurement of the distortion of the ^{8}B spectrum [1, 15], because the present positive 1σ signal could be produced by a $\Phi_{\rm hep}/\Phi_{^8{\rm B}}$ ratio 15 times larger than the prediction of BP95 [2]. Without a very large hep flux, the present measurement excludes an otherwise allowed region with $\Delta m^2 \approx 10^{-4}\,{\rm eV}^2$ and $\sin^2 2\theta_{12}$ in the range $10^{-4} \div 10^{-1}$ [13, 16].

Our model independent analysis allows us to investigate how well present experiments are able to measure the SSM-independent neutrino fluxes $\Phi_{^8{\rm B}}$ and $\Phi_{^7{\rm Be}}$. This question is answered in fig. 4, where we plot the values of the fluxes that can give a good ($\chi^2_8 < 6$) or very good ($\chi^2_8 < 3$) fit for *some* value of the oscillation parameters Δm^2_{12}, θ_{12} and θ_{13}. We see that the value of $\Phi_{^8{\rm B}}$ is currently determined with an error larger than the solar model expectation. It will be directly measured in the new on-going SNO experiment. On the contrary the value of $\Phi_{^7{\rm Be}}$ is at present totally unknown: in fact in the small angle MSW solution the monochromatic ^{7}Be flux can be completely converted into $\not{e}$ neutrinos, that are not detected by existing experiments. Borexino will be able to detect neutral currents effects in this range of energies and probably allow a direct determination of $\Phi_{^7{\rm Be}}$ [13].

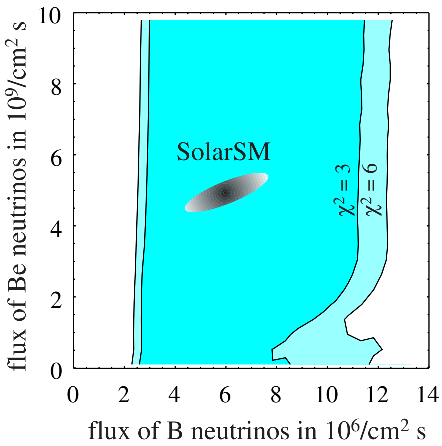

Figure 4: Isoplot of χ^2_8, minimized in the mixing parameters.

As discussed above we perform our analysis under the assumption that Δm^2_{23} is large enough that its effects decouple. For any given Δm^2_{23} it is straightforward to reproduce fig. 3 by using the exact expressions for $\theta^{\rm m}_{12}$ and $\theta^{\rm m}_{13}$ in equation (2.6). In this way we find that for small θ_{13} ($\lesssim 15°$), our results are insensitive to Δm^2_{23} down to $\Delta m^2_{23} = 5\cdot 10^{-4}\,{\rm eV}^2$. For large θ_{13}, Δm^2_{23} effects start to become noticeable when Δm^2_{23} drops below $2\times 10^{-3}\,{\rm eV}^2$; for example, for $\theta_{13} = 40°$ and $\Delta m^2_{23} = 5\cdot 10^{-4}\,{\rm eV}^2$, the allowed region in the SM inspired analysis is significantly smaller than in the decoupled limit, with the $\chi^2_{\rm min} < 6$ region never reaching $\sin^2(2\theta_{12}) > 0.1$. In spite of these changes for small Δm^2_{23}, the essential features of fig. 3 in any case remain unchanged.

2.2 Model independent solar analysis — one experiment ignored

In subsection 2.1, the present level of experimental evidence allowed us to omit one restriction (the solar model) and still yield interesting results. Likewise, we can choose to omit one experiment from the analysis while keeping some solar information and still yield interesting results.

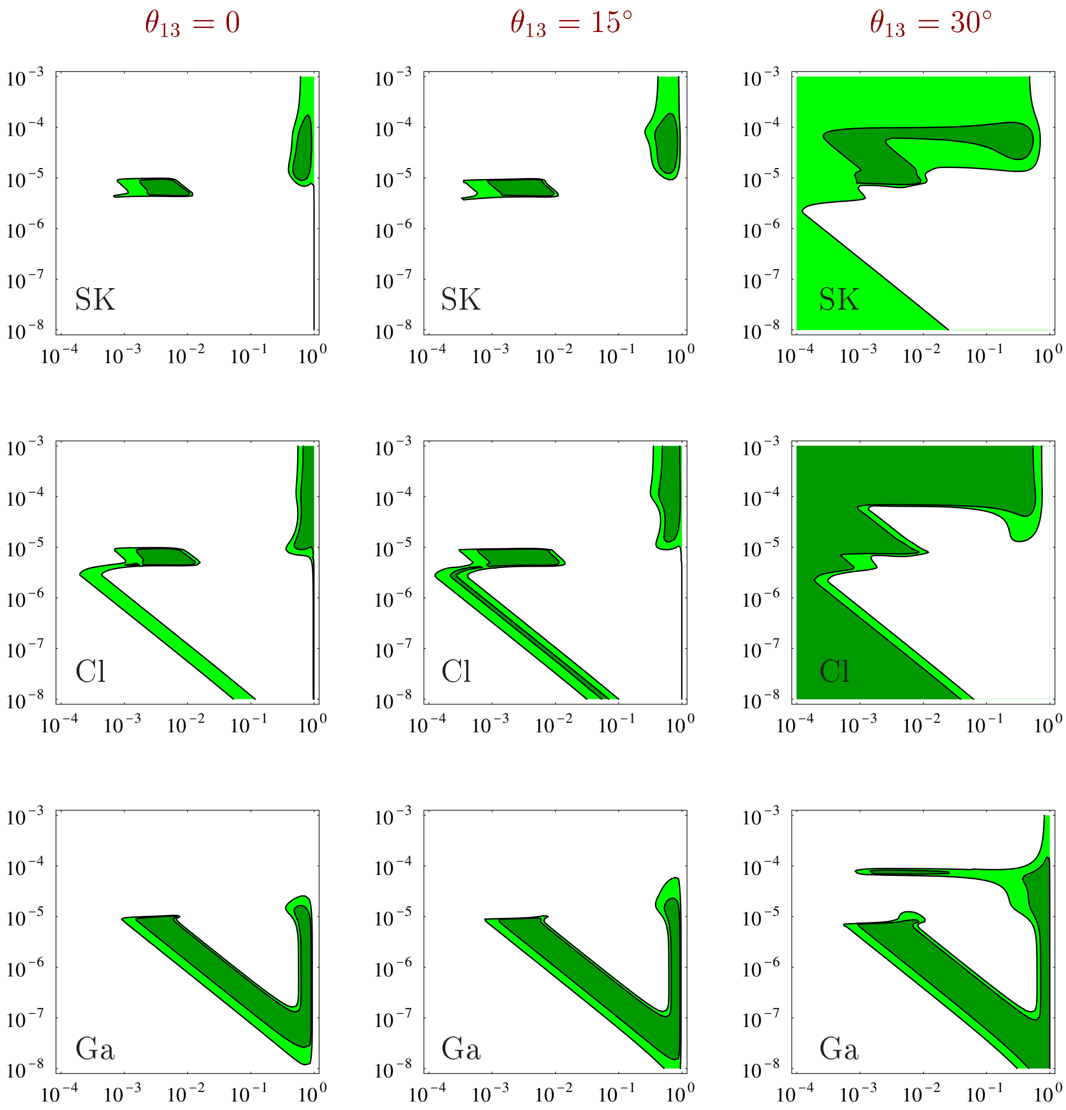

Figure 5: Fits of the solar data in the plane $(\sin^2 2\theta_{12}, \Delta m^2_{12}/\,\mathrm{eV}^2)$ for $\theta_{13} = 0, 15°$ and $30°$ assuming that one of the three solar neutrino experiments has a large unknown systematic error (SuperKamiokande in the first row, Chlorine in the second and Gallium in the third) and is therefore discarded from the analysis. The contours are for $\chi^2 = 3$ and $\chi^2 = 6$.

The motivation for this is obvious: neutrino experiments are extremely difficult to perform and particular detection schemes may suffer from some systematic error previously not considered. We make no judgements here about the errors associated with any particular experiment. Instead we consider analyses where we do not include one class of experiment, either water-Cerenkov, gallium or chlorine, which we designate $\not{\mathrm{SK}}$, $\not{\mathrm{Cl}}$ and $\not{\mathrm{Ga}}$ respectively. However, because we are losing an experiment, it is impossible to analyze the data without some level of information regarding the solar model. Consequently, we perform the analysis only within the solar SM inspired region. The results for this analysis are shown in figures 5 (upper row: without SuperKamiokande data, middle row: without chlorine data, and lower row: without gallium data).

The $\not{\mathrm{SK}}$ case largely resembles the complete data set analysis, with some additional space allowed in the higher Δm^2_{12} region. In contrast, the other two cases ($\not{\mathrm{Ga}}$ and $\not{\mathrm{Cl}}$) show considerable differences.

For the $\not{\mathrm{Ga}}$ case, there is a strong preference for either small Δm^2_{12} or large θ_{12} and θ_{13}. For the $\not{\mathrm{Cl}}$ case, for both large θ_{12} and θ_{13} we have the presence of large regions with large $\Delta m^2_{12} = 10^{-4}\,\mathrm{eV}^2$, above the level-crossing threshold, and with small Δm^2_{12}, in the non-adiabatic region. In either case, in a large portion of these regions matter enhancements are unimportant. That is, in the absence of one of these two classes of experiment, given sufficiently large angles, the solar neutrino problem can be resolved *simply by vacuum oscillations alone!* In such a case, new experiments, such as Borexino, would see an absence of energy dependence in the electron neutrino survival probability.

3. Atmospheric and solar neutrinos: the minimal scheme

The simplest picture for reconciling both solar and atmospheric neutrino fluxes via oscillations of $\nu_{e,\mu,\tau}$ results when there is a hierarchy $|\Delta m^2_{23}| \gg |\Delta m^2_{12}|$, and Δm^2_{12} is too small to affect oscillations of atmospheric neutrinos. In section 2, we showed that in this case the solar fluxes depend only on Δm^2_{12}, θ_{12} and θ_{13},[2] and below we show that the atmospheric fluxes depend only on $\Delta m^2_{23}, \theta_{23}$ and θ_{13}. In the limit that $\theta_{13} = 0$, the two phenomena become independent, in the sense that they depend on no common parameters: solar oscillations are $\nu_e \to \nu_\mu$ at a low frequency, while atmospheric oscillations are $\nu_\mu \to \nu_\tau$ at a much higher frequency. However, solar oscillations are allowed for a wide range of parameters with large θ_{13}, and the atmospheric data does not require θ_{13} to be very small. Hence, in this section we explore this simple picture keeping θ_{13} as a free parameter. We comment on the alternative possibility — that Δm^2_{12} is large enough to contribute to atmospheric neutrino oscillations — in section 4.

Matter effects in the earth are important only for a relatively small fraction of the atmospheric neutrinos, those with high energy, and they are neglected here.[3] In this case, (2.3) can be integrated to give oscillation probabilities $P_{ff'}(t) = |A_{ff'}(t)|^2$, where A is given by the matrix equation

$$A(t) = V e^{-iEt} V^\dagger\,. \tag{3.1}$$

Since an overall phase in A is irrelevant to P, and Δm^2_{12} effects are negligible, we

[2]Although for non-zero θ_{13}, there is a dependence on Δm^2_{23} if it is small enough.
[3]For more details see e.g. ref. [17].

JHEP12(1998)017

may make the substitution

$$e^{-iEt} \longrightarrow \text{diag}\left(1, 1, e^{-i\Delta m^2_{23}t/2E}\right) \tag{3.2}$$

Using the form (2.4) for V, we immediately discover that the probabilities are independent of θ_{12} and ϕ, as well as α and β. The probabilities are given by

$$\begin{aligned} P_{e\mu} &= s^2_{23}\sin^2 2\theta_{13}\ S_{23}\,, && (3.3)\\ P_{e\tau} &= c^2_{23}\sin^2 2\theta_{13}\ S_{23}\,, && (3.4)\\ P_{\mu\tau} &= c^4_{13}\sin^2 2\theta_{23}\ S_{23}\,, && (3.5) \end{aligned}$$

or equivalently, by unitarity

$$\begin{aligned} P_{ee} &= 1 - \sin^2 2\theta_{13}\ S_{23}\,, && (3.6)\\ P_{\mu\mu} &= 1 - 4c^2_{13}s^2_{23}\left(1 - c^2_{13}s^2_{23}\right)\ S_{23}\,, && (3.7)\\ P_{\tau\tau} &= 1 - 4c^2_{13}c^2_{23}\left(1 - c^2_{13}c^2_{23}\right)\ S_{23}\,, && (3.8) \end{aligned}$$

where $S_{23} = \sin^2(\Delta m^2_{23}t/4E)$. The parameter Δm^2_{23} can be extracted from the data by fitting to the zenith angle distribution of the events. Here we concentrate on the determination of the parameters θ_{13} and θ_{23}. These can be extracted, independent of the value of Δm^2_{23}, if we assume that the downward going neutrinos have not oscillated, while the upward going neutrinos are completely oscillated, so that S_{23} is averaged to 0.5. In view of the reported angular distribution of the multi-GeV data for 1-ring e-like, 1-ring μ-like and partially contained (PC) events [3], this assumption appears to be valid, at least for angular cone sizes about the vertical which are not too large. For events of class i, which are induced by ν_e charged current, ν_μ charged current and neutral current interactions with relative probabilities $f^i_{eCC}, f^i_{\mu CC}$ and f^i_{NC}, the up-down ratio ρ_i is given by

$$\rho_i = \frac{N_i^\uparrow}{N_i^\downarrow} = f^i_{eCC}\cdot(P_{ee} + rP_{e\mu}) + f^i_{\mu CC}\cdot\left(P_{\mu\mu} + \frac{1}{r}P_{e\mu}\right) + f^i_{NC}. \tag{3.9}$$

where we have set $S_{23} = 0.5$, and $N_i^{\uparrow,\downarrow}$ are the number of upward and downward events of class i. We are interested in i being 1-ring e-like, 1-ring μ-like and PC. The overall normalization of these event numbers has considerable uncertainties due to the calculation of the neutrino fluxes produced in cosmic ray showers, hence we consider three up-down ratios

$$\begin{aligned} \rho_e &= 1.23 \pm 0.29\,, && (3.10)\\ \rho_\mu &= 0.62 \pm 0.16\,, && (3.11)\\ \rho_{PC} &= 0.48 \pm 0.12\,, && (3.12) \end{aligned}$$

and two ratios of downward going fluxes

$$\frac{N_\mu^\downarrow + N_{PC}^\downarrow}{N_e^\downarrow} = \xi r = 3.0 \pm 0.6\,, \qquad \frac{N_{PC}^\downarrow}{N_\mu^\downarrow} = \xi' = 1.3 \pm 0.3\,, \tag{3.13}$$

where r is the ratio of ν_μ to ν_e fluxes. The numbers give the Super-Kamiokande data,

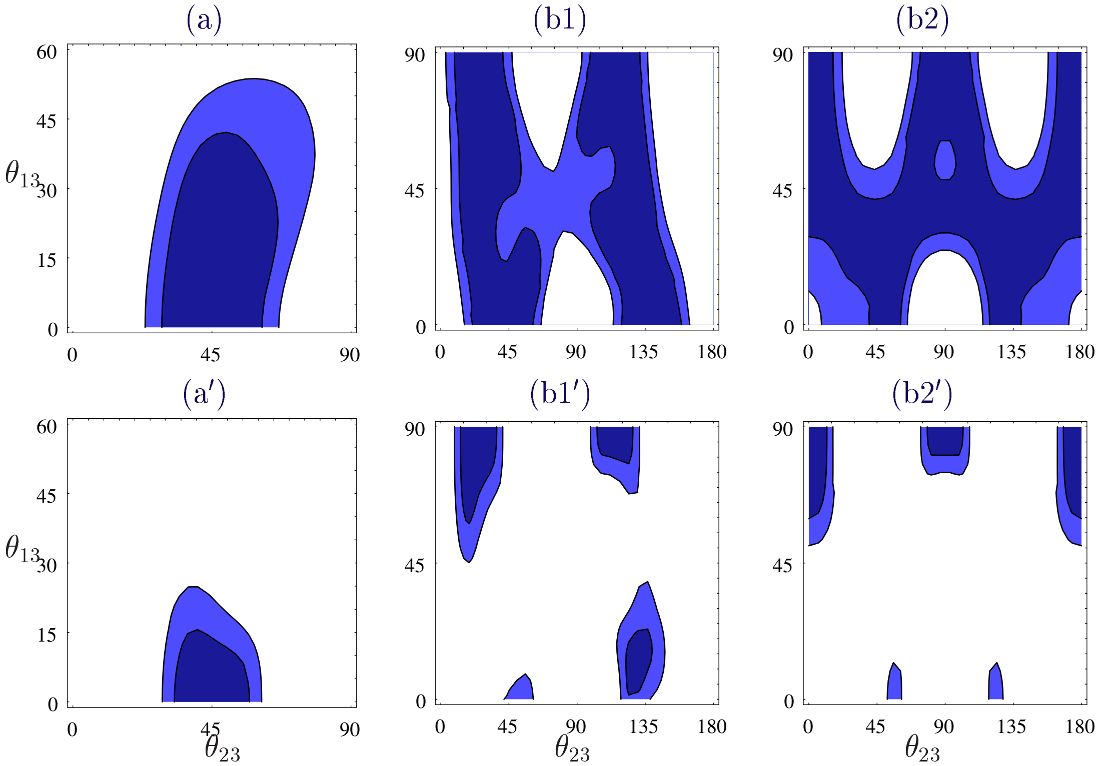

Figure 6: Mixing angles θ_{ij} that fit the up/down ratios (3.10) – (3.12) of atmospheric neutrinos, assuming that (a) $\Delta m^2_{12} \ll 10^{-3}\,\mathrm{eV}^2$ and any θ_{12}, (b) $\Delta m^2_{12} \approx \Delta m^2_{23} \approx 10^{-3}\,\mathrm{eV}^2$, $\phi = 0$ and (b1) $\theta_{12} = 20°$, (b2) $\theta_{12} = 45°$. Primed figures are as above, but including in the asymmetry also the intermediate bins in the angular distribution of [3] (see text). The contours are for $\chi^2 = 3$ and $\chi^2 = 6$.

extracted from the figures of ref. [3], with upward and downward directions defined by the azimuthal angle having $\cos\theta$ within 0.4 of the vertical direction. The parameters ξr and ξ' represent the theoretical values for the ratios of (3.13) and (3.13). These two downward going ratios do not involve oscillations, and the Super-Kamiokande collaboration compute Monte Carlo values of 3.1 and 1.0, respectively, agreeing very well with the data. Since these two ratios do not probe oscillations, at least within our assumptions, we do not use them for the fits below. We do not use the sub-GeV data as the poor angular correlation between the neutrino and charged lepton directions leads to a smoothing of the up-down ratio. From the flux calculations of Honda et al. [18], and using the measured momentum distributions for the events [3], we estimate $r = 4.0 \pm 0.5$, for this multi-GeV data near the vertical direction. A more refined analysis would use a larger value of r for PC events than for FC events.

The results of a fit of the three up/down ratios to the two free parameters θ_{23} and θ_{13} are shown in figure 6(a). We have obtained the fractions $f^i_{eCC,\mu CC,NC}$ from the Monte Carlo results of the Super-Kamiokande collaboration [3], and we have used the oscillation probabilities of (3.5). In order to work with Gaussian distributed experimental data, we have directly fitted the six measured neutrino numbers $N_i^{\uparrow,\downarrow}$ leaving arbitrary the three overall fluxes of each type, $N_i^{\uparrow} + N_i^{\downarrow}$. The preferred region of the plot is easy to understand, since at the point $\theta_{23} = 45°$ and $\theta_{13} = 0$, the ν_e are unmixed, while there is complete $\nu_\mu \leftrightarrow \nu_\tau$ mixing, so $\rho_e \simeq 1$ and $\rho_\mu \simeq \rho_{PC} \simeq 0.5$. It is apparent from fig. 6(a) that this minimal scheme is allowed for a large range of angles about this point: $\theta_{23} = 45° \pm 15°$ and $\theta_{13} = 0 \div 45°$.

If the solar neutrino fluxes, measured by all three techniques, are to agree with solar model inspired values, then the results of section 2 show that Δm^2_{12} is too small to affect atmospheric oscillations, it is either of order $10^{-4} - 10^{-5}\,\mathrm{eV}^2$ or of order $10^{-10}\,\mathrm{eV}^2$. In this case, the minimal scheme for atmospheric neutrinos, described in this section, is the unique possibility using just the three known neutrinos. This observation enhances the importance of the fit of figure 6(a); further data will reduce the allowed region, as the three up-down ratios of (3.12) have small systematic uncertainties and are statistics limited. The solar neutrino fluxes do not put extra constraints on the value of θ_{13}, although it becomes correlated with θ_{12}, as shown in figure 3. If the atmospheric flux measurements require $\Delta m^2_{23} > 2 \times 10^{-3}\,\mathrm{eV}^2$, then the limit on P_{ee} from the CHOOZ experiment [19] requires $\theta_{13} < 13°$.

Recent analyses [20] of SuperKamiokande data that make use of MonteCarlo predictions for the angular and energy distributions of the atmospheric neutrinos get more stringent constraints on the neutrino oscillation parameters. Our fit uses only those data — the ratio of upward and downward multi-GeV neutrinos (the ones in bins 1 and 5 of the angular distribution in [3]) — that do not depend on the spectrum of the atmospheric neutrinos nor on the precise value of Δm^2, assuming a full averaged oscillation in between. Since statistics gives presently the dominant error, we obtain weaker constraints than in [20]. If we knew that the neutrino mass difference relevant for atmospheric neutrinos were close to the center of the presently allowed region, we could add to the data to be fitted the intermediate bins 2 and 4 of [3] (the bins that contain 'oblique' neutrinos). We cannot use in any case the multi-GeV data in the intermediate bin 3, that contains 'horizontal' neutrinos. Having doubled the statistics, we would find the more stringent contours shown in fig. 6a$'$, b1$'$, b2$'$. We remind the reader that our fit does not include matter effects [4].

4. Atmospheric and solar neutrinos: non-minimal schemes

In this section, we study atmospheric neutrinos when two conditions apply.

1. The smallest mass splitting is large enough to affect atmospheric neutrino oscillations: $\Delta m^2_{12} > 3 \times 10^{-4}\,\mathrm{eV}^2$. For solar neutrinos, this implies that there is a serious flaw either in at least one measurement technique, or in the solar models.

2. The mass splittings are hierarchical $\Delta m^2_{23} \gg \Delta m^2_{12}$. This is a simplification, which we relax at the end of the section. It includes the interesting possibility that Δm^2_{23} is large enough to induce the apparent oscillations reported by the LSND collaboration [21], while Δm^2_{12} effects are causing both solar and atmospheric oscillations.

Using (2.5), the ν_e survival probability is

$$P_{ee} = 1 - c^4_{13} \sin^2 2\theta_{12}\ S_{12} - s^2_{12} \sin^2 2\theta_{13}\ S_{23} - c^2_{12} \sin^2 2\theta_{13}\ S_{31}\,, \qquad (4.1)$$

where $S_{ij} = \sin^2(\Delta m^2_{ij} t/4E)$. The above two conditions imply that $\Delta m^2_{23} > 2 \times 10^{-3}\,\mathrm{eV}^2$, so that, for the CHOOZ experiment, (4.1) should be used with $S_{23} = S_{31} = 0.5$. The CHOOZ limit, $P_{ee} > 0.9$, then gives $\theta_{13} < 0.23$. If Δm^2_{12} were also greater than $2 \times 10^{-3}\,\mathrm{eV}^2$, then for the CHOOZ experiment one also has $S_{12} = 0.5$, so that $\theta_{12} < 0.23$. However, in this case the survival probability for solar neutrinos is the same as for the anti-neutrinos at CHOOZ: $P_{ee} > 0.9$. Hence, given our two conditions, the observed solar neutrino fluxes require $\Delta m^2_{12} < 2 \times 10^{-3}\,\mathrm{eV}^2$.

It is frequently stated that the three known neutrinos cannot explain the LSND, atmospheric and solar neutrino anomalies, as this would require three Δm^2 with different orders of magnitudes. However, this argument no longer applies in the case that either a solar neutrino measurement technique or solar models are incorrect, when a single Δm^2 could give both atmospheric and solar anomalies. Hence, we consider first the case that Δm^2_{23} is large enough to explain the observations of LSND. The oscillation probabilities induced by Δm^2_{23} are given by (3.5). From the limit on P_{ee} from the Bugey reactor, one then concludes

$$\Delta m^2_{23} > 0.2\,\mathrm{eV}^2\,, \qquad (4.2)$$

and

$$\theta_{13} < 0.1\,, \qquad (4.3)$$

which is significantly stronger than the CHOOZ limit. A second possibility, θ_{13} close to 90° does not allow any significant oscillations of ν_e and is thus not acceptable to explain the solar neutrino anomaly at a relatively large frequency. For atmospheric neutrinos, both upward going and downward going, one may then use oscillation probabilities with $\theta_{13} = 0$,[4] and with S_{23} and S_{13} both averaged to 0.5:

$$P_{e\mu} = c^2_{23} \sin^2 2\theta_{12}\ S_{12}\,, \qquad (4.4)$$
$$P_{e\tau} = s^2_{23} \sin^2 2\theta_{12}\ S_{12}\,, \qquad (4.5)$$
$$P_{\mu\tau} = -\tfrac{1}{4} \sin^2 2\theta_{23} \sin^2 2\theta_{12}\ S_{12} + \tfrac{1}{2} \sin^2 2\theta_{23}\,, \qquad (4.6)$$

[4]In which case the P_{ij} are independent of ϕ.

JHEP12(1998)017

or equivalently, from unitarity

$$P_{ee} = 1 - \sin^2 2\theta_{12}\, S_{12}\,, \tag{4.7}$$
$$P_{\mu\mu} = 1 - \tfrac{1}{2}\sin^2 2\theta_{23} - c_{23}^4 \sin^2 2\theta_{12}\, S_{12}\,, \tag{4.8}$$
$$P_{\tau\tau} = 1 - \tfrac{1}{2}\sin^2 2\theta_{23} - s_{23}^4 \sin^2 2\theta_{12}\, S_{12}\,. \tag{4.9}$$

Since in these formulæ $S_{13} = S_{23}$, θ_{12} enters only via $\sin^2 2\theta_{12}$ so that, without loss of generality, we may reduce the range of θ_{12} to $0 \le \theta_{12} < \pi/4$. We again study the up-down ratios (3.9), as they have small systematic uncertainties. We calculate them approximately, using (3.9) with $f^e_{eCC} = f^\mu_{\mu CC} = f^{PC}_{\mu CC} = 1$ and all other f-factors equal to zero. A fraction, $P^{(0)}_{\mu\mu} = 1 - \sin^2 2\theta_{23}/2$, of the downward going ν_μ oscillate to ν_τ before detection, so the up-down ratios are given by

$$\rho_e \approx P_{ee} + r P_{e\mu} \tag{4.10}$$

and

$$\rho_\mu \approx \frac{P_{\mu\mu} + P_{e\mu}/r}{P^{(0)}_{\mu\mu}}\,. \tag{4.11}$$

Hence we find

$$(\rho_\mu - 1) \approx -\frac{1}{r}\frac{c_{23}^2}{1 - \frac{1}{2}\sin^2 2\theta_{23}} \cdot (\rho_e - 1)\,. \tag{4.12}$$

For the multi-GeV data, where the angular correlation is best, r is large, and (4.12) implies that $|\rho_\mu - 1| < (1/3)|\rho_e - 1|$, in strong disagreement with data of (3.12). The same inequality holds if ρ_μ is replaced by ρ_{PC}, when the disagreement with data is even stronger.[5] *With oscillations of the three known neutrinos, the LSND observation conflicts with the atmospheric and solar neutrino anomalies even using a model independent analysis of the solar neutrino fluxes or allowing for a systematic error in one of the solar neutrino experiments.*[6]

Does the atmospheric neutrino data allow other values of $\Delta m^2_{23} \gg \Delta m^2_{12}$? The limit from the Bugey reactor, (4.3), applies for all $\Delta m^2_{23} > 0.06\,\mathrm{eV}^2$, and the up-down ratio relation, (4.12), applies for all $\Delta m^2_{23} > 0.1\,\mathrm{eV}^2$. Hence, $\Delta m^2_{23} > 0.1\,\mathrm{eV}^2$ is excluded. For $\Delta m^2_{23} < 0.1\,\mathrm{eV}^2$, the downward going ν_μ have not oscillated to ν_τ when they reach the Super-Kamiokande detector, so that (4.11) is replaced by

$$\rho_\mu \approx P_{\mu\mu} + \frac{1}{r}P_{e\mu} = 1 - \frac{1}{2}\sin^2 2\theta_{23} - \frac{c_{23}^2}{r}(\rho_e - 1)\,. \tag{4.13}$$

Consistency with the data, (3.12), is now possible, and requires large θ_{23}. As Δm^2_{23} drops below $0.06\,\mathrm{eV}^2$, the limit from the Bugey reactor on θ_{13} is progressively weakened, so that θ_{13} terms must be kept in P_{ij}. Furthermore, as Δm^2_{23} drops below

[5] Even ignoring ρ_e, we find $\rho_{PC,\mu} > 0.61$.

[6] For $\theta_{23} = 0$, this corresponds to purely $\nu_\mu \to \nu_e$ oscillations, which is therefore excluded as an explanation of the atmospheric neutrino measurements.

JHEP12(1998)017

$0.01\,\mathrm{eV}^2$, our hierarchy condition is no longer satisfied, so that P_{ij} depend also on θ_{12}. For these cases we have performed a χ squared fit of the three up-down ratios (3.12) to θ_{23}, θ_{13} and θ_{12}, for various values of the mass splittings, and have found acceptable regions of parameter space. Results are shown in figure 6b for the case that all $S_{ij} = 0$ for downward going neutrinos, while all $S_{ij} = 0.5$ for upward going neutrinos and $\phi = 0$ (no CP violation). An equivalent fit would be obtained for $\phi = \pi$ and $\theta_{23} \to \pi - \theta_{23}$. The (relatively small) asymmetry of figs. 6b under $\theta_{23} \to \pi - \theta_{23}$ shows the dependence on ϕ of the SuperKamiokande data considered here.

A comparison of figure 6b with figures 3 and 5 shows under what conditions this large Δm^2_{12} scheme gives consistency. If all solar measurement techniques are correct, then, from figure 3, θ_{13} is small and $\theta_{12} = 10^\circ \div 20^\circ$. Figure 6b then shows that θ_{23} is centred on $45^\circ \pm 25^\circ$, the range around $\theta_{23} = 135^\circ$ being equivalent for any ϕ since θ_{13} is small. Figure 5 shows that solar model inspired fits to data from two solar techniques at large Δm^2_{12} allow larger ranges of θ_{12} and θ_{13}, and these become correlated with θ_{23} via figure 6b.

5. Large $\nu_\mu \to \nu_\tau$ mixing for atmospheric neutrinos

The pattern of masses and mixings suggested by the previous considerations show peculiar features, especially if both the atmospheric and solar neutrino anomalies are accounted for in the minimal scheme of section 3. The mass differences are hierarchical. However a large mixing ($\theta_{23} \approx 45^\circ$) is required between the states with the *largest* mass difference. The mixing angle θ_{12} between the states with the *smallest* mass splitting may be large or small. Finally, if $\Delta m^2_{\rm atm} \geq 2 \cdot 10^{-3}\,\mathrm{eV}^2$, i.e. in the CHOOZ range, the third mixing angle must be small, $\theta_{13} \leq 13^\circ$. Therefore it looks interesting to see which mass matrix could produce this pattern and which flavour symmetries can justify it.

5.1 2×2 matrix forms

As stressed in the introduction, an important consequence of the data on atmospheric neutrino fluxes is the need for large mixing angles. Here we study four possible forms of the 2×2 Majorana mass matrix for ν_μ and ν_τ which have a large mixing angle. In subsection 5.2 we study whether these forms can be incorporated in 3×3 mixing schemes which also give solar neutrino oscillations, and whether 3×3 cases exist which cannot be reduced to a 2×2 form. In section 6 we study whether these forms may be obtained from flavour symmetries of abelian type.

In a basis with a diagonal charged lepton mass matrix, the Majorana neutrino mass matrix is

$$m = \frac{v^2}{M} \begin{pmatrix} C & B \\ B & A \end{pmatrix}. \tag{5.1}$$

	small entries	small parameters	order unity parameters	$\frac{\Delta m^2}{(\frac{v^2}{M})^2}$
(1) Generic	none	none	A, B, C	≈ 1
(2) Determinant small	none	none	$A, B, C = \frac{B^2}{A} + \varepsilon$	≈ 1
(3) One diagonal small	one diagonal	$C \approx \varepsilon$	A, B	≈ 1
(4) Pseudo-Dirac	both diagonal	$A, C \approx \varepsilon$	B	$\approx \varepsilon$

Table 1: The four possible 2×2 matrix forms which give a large mixing angle.

This is brought into real, diagonal form by the unitary matrix

$$V = R(\theta) \begin{pmatrix} 1 & 0 \\ 0 & e^{i\alpha} \end{pmatrix}, \tag{5.2}$$

where $\tan 2\theta = 2B/(A - C)$, and the phase α does not affect oscillations. The mass difference relevant for oscillations is $\Delta m^2 = (A + C)\sqrt{(A - C)^2 + 4B^2}$. The coefficient v^2/M is motivated by the see-saw mechanism, with v the electroweak vacuum expectation value and M the mass of a heavy right-handed neutrino.

There are four possible forms of this matrix which give $\theta \approx 1$, and these are shown in table 1. In cases (1) and (2) the entries are all of order unity; in the generic case they are unrelated, while in case (2) they are related in such a way that the determinant is suppressed. We discuss how such a suppression can occur naturally via the seesaw mechanism in the next section. Case (3) has one of the diagonal entries suppressed, which, however, does not follow from a simple symmetry argument. For cases (1÷3), taking $\Delta m^2 = 10^{-3}\,\mathrm{eV}^2$, one finds

$$M = (1 \div 3) \times 10^{15}\mathrm{GeV}\,, \tag{5.3}$$

close to the scale of gauge coupling unification in supersymmetric theories.

Finally, case (4) has both diagonal entries small, making ν_μ and ν_τ components of a pseudo-Dirac neutrino. This follows from an approximate $L_\mu - L_\tau$ symmetry, and implies that $\theta \simeq 45°$. This agrees well with data: combing ρ_μ and ρ_{PC} of (3.12) gives $\theta = 45° \pm 15°$. Of the four possible cases with large mixing angle, it is only the pseudo-Dirac neutrino which allows $\nu_{\mu,\tau}$ to be the astrophysical hot dark matter, in which case one predicts $\theta = 45°$ to high accuracy.

From the viewpoint of atmospheric neutrino oscillations alone, the distinction between cases (1) and (2) is unimportant. Since case (3) does not follow from simple symmetry arguments, one is left with two main 2×2 mixing schemes: the generic and pseudo-Dirac cases.

5.2 3×3 matrix forms

There are many possibilities for 3×3 neutrino mixing giving $P_{\mu\mu} \approx 0.5$, with oscillation primarily to ν_τ. In general two independent frequencies and three Euler angles are involved.

For the case that the oscillation is dominated by a single frequency, the possibilities may be divided into two classes: "2×2-like" and "inherently 3×3." The 2×2-like cases are just the four discussed in subsection 5.1, with $\theta_{12,13}$ small. Even though Δm^2_{23} may not be the largest Δm^2, it is the only one which causes substantial depletion of ν_μ. More interesting are the inherently 3×3 cases, for which there is no 2×2 reduction.

Consider the case

$$m = \frac{v^2}{M} \begin{pmatrix} 0 & B & A \\ B & 0 & 0 \\ A & 0 & 0 \end{pmatrix}, \tag{5.4}$$

with $A, B \approx 1$. This is diagonalized by $V = R_{23}(\theta_{23}) R_{12}(\theta_{12} = 45^\circ)$ giving a Dirac state of ν_e married to $c_{23}\nu_\mu + s_{23}\nu_\tau$. The mass eigenvalues are $(M, M, 0)$, which, from the viewpoint of oscillations are equivalent to $(0, 0, M)$. Hence, one immediately sees that the oscillation probabilities are given by (3.5) with $\theta_{13} = 0$: $P_{\mu\tau} = \sin^2 2\theta_{23} S_{23}$ has the form of a 2×2 oscillation, even though the mass matrix has an inherently 3×3 form. This arises because (5.4) is governed by the symmetry $L_e - L_\mu - L_\tau$, which allows $\nu_\mu \leftrightarrow \nu_\tau$, but prevents ν_e from oscillating.

We claim that (5.4) is the only inherently 3×3 form for $\nu_\mu \rightarrow \nu_\tau$ *at a single frequency*, as we now show. An inherently 3×3 form must have large entries outside the 2×2 block in 23 subspace. The three possibilities are 11, 12 and 13 (and their symmetric). None of these entries work alone, even coupled to any structure in the 23 block: either one gets two comparable frequencies or one does not get $\nu_\mu \rightarrow \nu_\tau$. The same is true for 11 + 12 or 11 + 13, again possibly together with any 23-block. Since 11 + 12 + 13 leads to two comparable frequencies, the only case remaining is 12 + 13, with a relatively negligible 23 block, i.e. the 3×3 form in (5.4). Basic to this conclusion is the assumption of no special relations among the different neutrino matrix elements other than the symmetry of the matrix itself (for alternatives see [22]).

6. Models for both solar and atmospheric neutrinos

In this section we construct models for the minimal scheme for atmospheric and solar neutrino oscillations, discussed in section 3. The mass pattern suggested by this scheme has the hierarchy $\Delta m^2_\odot \equiv \Delta m^2_{12} \ll \Delta m^2_{\rm atm} \equiv \Delta m^2_{23}$. We take the form of the lepton mass matrices to be determined by flavour symmetries (FS) and assume that all small entries in these matrices are governed by small flavour symmetry breaking (FSB) parameters.

The low energy effective mass matrix for the three light left-handed neutrinos can be written as the sum of two matrices: $m_{LL} = m_{\rm atm} + m_{\odot}$, where all non-zero entries of $m_{\rm atm}$ are larger than all entries of $m_{\odot}$. The form of $m_{\rm atm}$ is such that there is a large mass splitting: $\Delta m^2_{\rm atm} \approx 10^{-(2\div 3)}\,{\rm eV}^2$, and a vanishing Δm^2. Furthermore, this matrix must give a large depletion of ν_μ, and, as discussed in the last section, this could occur if it has certain 2×2-like or inherently 3×3 forms. Of the two 2×2-like forms shown in Table 1, only case (2) is acceptable: in cases (1) and (3) the two independent Δm^2 are comparable, while in case (4) the second independent Δm^2 is larger than $\Delta m^2_{\rm atm}$. Hence, we arrive at the possibility:[7]

$$m^{2\times 2}_{\rm atm} = \frac{v^2}{M}\begin{pmatrix} 0 & 0 & 0 \\ 0 & C & B \\ 0 & B & A \end{pmatrix}, \tag{6.1}$$

with $A, B \approx 1$ and $C = B^2/A$. A reason for the vanishing sub-determinant will be given shortly.

In the previous section we have proved that there is a unique form for $m_{\rm atm}$ which is inherently 3×3:

$$m^{3\times 3}_{\rm atm} = \frac{v^2}{M}\begin{pmatrix} 0 & B & A \\ B & 0 & 0 \\ A & 0 & 0 \end{pmatrix}, \tag{6.2}$$

with $A, B \approx 1$.

The oscillation angles in the leptonic mixing matrix, V, have contributions from diagonalization of both the neutrino mass matrix, θ^ν_{ij}, and the charged lepton mass matrix, θ^e_{ij}: $V(\theta_{ij}) = V^{e\dagger}(\theta^e_{ij})V^\nu(\theta^\nu_{ij})$. This requires discussing also the charged lepton mass matrix. It is not easy to construct an exhaustive list of the possible symmetries and their breaking parameters. This is partly because there are both discrete and continuous symmetries with many choices for breaking parameters; but is mainly because of a subtlety of the seesaw mechanism. Let m_{RR} and m_{LR} be the most general Majorana and Dirac mass matrices of the seesaw mechanism allowed by some approximate symmetry. On forming the mass matrix for the light states, $m_{LL} = m_{LR} m^{-1}_{RR} m^T_{LR}$, one discovers that m_{LL} need not be the most general matrix allowed by the approximate symmetry. This means that one cannot construct an exhaustive list by only studying the symmetry properties of m_{LL} — it is necessary to study the full theory containing the right-handed states.

A casual glance at (6.1) and (6.2) shows that the flavor symmetry we seek, from the viewpoint of $\Delta L = 2$ operators, does not distinguish l_μ from l_τ, but does distinguish these from l_e. There are many combinations of the three lepton numbers

[7] Ansätze of this type for the neutrino mass matrix, up to small corrections, to describe atmospheric and solar neutrinos are contained in refs [23].

L_a, and their subgroups, acting on l_a, which have this property. As representative of this group, we choose the combination $L_e - L_\mu - L_\tau$. We find it remarkable that this symmetry group can yield both (6.1) and (6.2), depending on how it is realized.

6.1 $L_e - L_\mu - L_\tau$ realized in the low energy effective theory

In the effective theory at the weak scale, we impose an approximate $L_e - L_\mu - L_\tau$ symmetry, which acts on the weak doublets, $l_{e,\mu,\tau}$, and is broken by small FSB parameters, ε and ε' of charge +2 and -2, respectively, giving a neutrino mass matrix:

$$m_{LL} = \frac{v^2}{M} \begin{pmatrix} \varepsilon' & 1 & 1 \\ 1 & \varepsilon & \varepsilon \\ 1 & \varepsilon & \varepsilon \end{pmatrix}. \tag{6.3}$$

Hereafter, the various entries of the matrices only indicate the corresponding order of magnitude, allowing for an independent parameter for each entry. This texture gives

$$m_1 \approx m_2 \approx \frac{v^2}{M}\ , \qquad \Delta m^2_{12} \approx \frac{v^4}{M^2}(\varepsilon + \varepsilon')\,, \tag{6.4}$$

$$m_3 \approx \frac{v^2}{M}\varepsilon\,, \qquad \Delta m^2_{23} \approx \frac{v^4}{M^2}\,, \tag{6.5}$$

and

$$\theta^\nu_{23} \approx 1\,, \qquad \theta^\nu_{13} \approx \varepsilon\,, \qquad \theta^\nu_{12} = 45^\circ\,. \tag{6.6}$$

While the texture gives only the order of magnitude of θ^ν_{23}, it precisely predicts θ^ν_{12} to be close to 45°. If the FSB parameters ε and ε' are taken to be extremely small, this becomes an excellent candidate for the case of "just so" solar neutrino oscillations, with the prediction that $\theta_{12} = 45^\circ$. However, from figure 3 it follows that this model cannot give matter neutrino oscillations in the sun, which requires $\sin 2\theta_{12} \leq 0.9$. There are several contributions to the deviation of $\sin 2\theta_{12}$ from unity, but they are all too small to reconcile the discrepancy. A hierarchy in Δm^2 requires $\varepsilon, \varepsilon' < 0.1$, and since $\sin^2 2\theta^\nu_{12} \simeq 1 - (\varepsilon - \varepsilon')^2/8$, the deviation of $\sin 2\theta^\nu_{12}$ from 1 is negligible. After performing the θ^ν_{12} rotation, there are small $\mathcal{O}(\varepsilon)$ rotations in the 13 and 23 planes necessary to fully diagonalize m_{LL}; these are too small to affect our conclusions. The last hope is that there could be a significant contribution to θ_{12} from diagonalization of the charged lepton mass matrix. As mentioned above, the diagonalization of the charged lepton mass matrix has to be discussed anyhow.

Consistently with the symmetry structure of (6.3), the most general form for the charged lepton mass matrix, with a structure governed by abelian symmetries is

$$m_E = \lambda v \begin{pmatrix} \xi' & \xi\varepsilon' & \varepsilon' \\ \xi'\varepsilon & \xi & 1 \\ \xi'\varepsilon & \xi & 1 \end{pmatrix}. \tag{6.7}$$

when left (right) handed leptons are contracted to the left (right), $\bar{e}_L m_E e_R$. $(1, \xi, \xi')$ are the relative FSB parameters of (τ_R, μ_R, e_R) with respect to some other approximate FS, needed to describe the charged lepton mass hierarchies, and λ is the absolute FSB parameter of $\bar{\tau}_R \tau_L$. Here we ignore the fact that non-abelian symmetries could modify this form, for example by requiring some entries to vanish.

Diagonalization of (6.7) leads to

$$\theta^e_{23} \approx 1\,, \qquad \theta^e_{13} \approx \varepsilon'\,, \qquad \theta^e_{12} \approx \varepsilon'\,.$$

Therefore, altogether

$$\theta_{23} \approx 1\,, \qquad \theta_{12} \approx \varepsilon + \varepsilon'\,, \qquad \theta_{12} \approx 45^\circ\,.$$

Since $\sin^2 2\theta_{12}$ remains corrected only by quadratic terms in ε and/or ε', we conclude that $L_e - L_\mu - L_\tau$, realized as an approximate symmetry of the low energy effective theory, can explain both atmospheric and solar neutrino fluxes with a hierarchy of Δm^2, most likely *only* for the case of "just so" vacuum solar oscillations, in which case the scale of new physics, M, is close to the gauge unification scale, and the FSB parameters are extremely small: $\varepsilon, \varepsilon' \approx 10^{-7}$. This result also applies when *any* approximate FS of the low energy effective theory yields (6.3). In view of (6.4) – (6.6), with $\Delta m^2_{23} \approx \Delta m^2_{\rm atm} \approx 10^{-(2\div 3)}\,\mathrm{eV}^2$, notice that all three neutrinos are cosmologically irrelevant. Furthermore, the smallness of the 11 entry of (6.3) makes the search for neutrino-less 2β-decay uninteresting.

Comparing the θ_{13} plots of figures 3 and 5, one finds that, with one experiment excluded, the case of $\theta_{12} = 45^\circ$ becomes allowed for a large range of Δm^2_{12}, giving another application for this inherently 3×3 form of the mass matrix.

6.2 $L_e - L_\mu - L_\tau$ realized via the seesaw mechanism

The seesaw mechanism [24] allows a simple origin for the vanishing of the 2×2 subdeterminant of (6.1). Consider a single right-handed neutrino, N, with Majorana mass M and Dirac mass term $vN(\cos\theta\nu_\tau + \sin\theta\nu_\mu)$, where $\theta \approx 1$. Integrating out this single heavy state produces a single non-zero eigenvalue in m_{LL} — giving (6.1) with $A = \cos^2\theta, B = \cos\theta\sin\theta$ and $C = \sin^2\theta$, so that $AC = B^2$.

How could this carry over to a theory with three right-handed neutrinos, N_a? As long as one of them, N with the above mass terms, is much lighter than the others, then it will give the dominant contribution to m_{LL}, which will have (6.1) as its leading term. Clearly the key is that there be one right-handed neutrino which is lighter than the others, and couples comparably to ν_μ and ν_τ.

This can be realized using $L_e - L_\mu - L_\tau$, with two small FSB parameters ε $(+2)$ and ε' (-2). The right-handed neutrino mass matrix is

$$m_{RR} = M \begin{pmatrix} \varepsilon' & 1 & 1 \\ 1 & \varepsilon & \varepsilon \\ 1 & \varepsilon & \varepsilon \end{pmatrix} \tag{6.8}$$

and the Dirac mass matrices of neutrinos and charged leptons are

$$m_{LR} = \lambda' v \begin{pmatrix} \eta' & \varepsilon\eta' & \varepsilon\eta' \\ \varepsilon'\eta & \eta & \eta \\ \varepsilon' & 1 & 1 \end{pmatrix} \qquad \text{and} \qquad m_E = \lambda v \begin{pmatrix} \xi'\eta' & \varepsilon\xi\eta' & \varepsilon\eta' \\ \xi'\varepsilon'\eta & \xi\eta & \eta \\ \xi'\varepsilon' & \xi & 1 \end{pmatrix}, \tag{6.9}$$

where, in analogy with eq. (6.7), we have introduced FSB parameters consistent with (6.8).

For ease of exposition, let us first consider the case where all the η and ξ factors are set equal to unity. The crucial point is that there is a massless right-handed neutrino in the limit $\varepsilon \to 0$. Hence, taking ε small, and doing a rotation in the 23 plane we have 2×2 sub-matrices

$$m_{RR}^{-1} = \frac{1}{M} \begin{pmatrix} 0 & 0 \\ 0 & 1/\varepsilon \end{pmatrix}, \qquad m_{LR} = \lambda' v \begin{pmatrix} 1 & 1 \\ 1 & 1 \end{pmatrix}, \tag{6.10}$$

giving

$$m_{LL} = \frac{(\lambda' v)^2}{M} \begin{pmatrix} 1/\varepsilon & 1/\varepsilon \\ 1/\varepsilon & 1/\varepsilon \end{pmatrix}, \tag{6.11}$$

where $\det m_{LL} = 0$ at this order. In a theory with right-handed neutrinos, $L_e - L_\mu - L_\tau$ leads to (6.1).

Extending the analysis to 3×3 matrices is straightforward. The inverse of m_{RR}

$$m_{RR}^{-1} = \frac{1}{M} \begin{pmatrix} \varepsilon & 1 & 1 \\ 1 & \varepsilon' & \varepsilon' \\ 1 & \varepsilon' & \frac{1}{\varepsilon} \end{pmatrix}, \tag{6.12}$$

shows a pseudo-Dirac structure in the 12 subspace, which is preserved in the light neutrino mass matrix:

$$m_{LL} = \frac{(\lambda' v)^2}{M} \begin{pmatrix} \varepsilon & 1 & 1 \\ 1 & \varepsilon' & 0 \\ 1 & 0 & \frac{1}{\varepsilon} \end{pmatrix}, \tag{6.13}$$

where we have gone to a basis which diagonalizes the 23 subspace. The parameters relevant for neutrino oscillation are

$$\theta_{23}^{e,\nu} \approx 1\,, \qquad \theta_{13}^{e,\nu} \approx \varepsilon\,, \qquad \theta_{12}^{\nu} = 45^\circ\,, \qquad \theta_{12}^{e} \approx \varepsilon \tag{6.14}$$

and

$$\Delta m_{23}^2 \approx \frac{1}{\varepsilon^2}\frac{(\lambda' v)^4}{M^2}\,, \qquad \Delta m_{12}^2 \approx (\varepsilon + \varepsilon')\frac{(\lambda' v)^4}{M^2}\,. \tag{6.15}$$

It is remarkable that $L_e - L_\mu - L_\tau$ has forced a pseudo-Dirac structure in the 12 subspace as in its previous realization, again giving θ_{12} near 45°. The crucial difference is that the pseudo-Dirac mass splitting is now a higher power in FSB than before

$$\frac{\Delta m_{12}^2}{\Delta m_{23}^2 \approx \varepsilon^2(\varepsilon + \varepsilon')\,,} \tag{6.16}$$

rather than $\varepsilon + \varepsilon'$. This allows ε and ε' to be considerably larger than before, so $\sin 2\theta_{12} < 0.8$ is now possible, allowing large angle MSW solar neutrino oscillations. In this case the FSB parameters are not very small $\varepsilon, \varepsilon' \approx 0.3 \div 0.5$, so that the mass of the right-handed neutrinos is still quite close to the gauge coupling unification scale. Notice again the cosmological irrelevance of the neutrino masses. For neutrino-less 2β decay searches $(m_{LL})_{11} \approx \epsilon^3 (\Delta m^2_{23})^{1/2} \leq 10^{-2}\,\mathrm{eV}^2$. Finally, $\varepsilon' \approx 0.1$ and $\lambda' \approx 1$ can make M exactly coincident with the unification scale.

So far we have only produced models with large θ_{12}. However $L_e - L_\mu - L_\tau$ realized with the seesaw mechanism may also lead to small θ_{12}, using the FSB suppression factors in (6.9). Taking $\eta' \ll \varepsilon'$ and $\eta \approx 1$, in an appropriate 23 basis gives

$$m_{LL} = \frac{(\lambda' v)^2}{M} \begin{pmatrix} {\eta'}^2 \varepsilon & \eta' & \eta' \\ \eta' & \varepsilon' & 0 \\ \eta' & 0 & \frac{1}{\varepsilon} \end{pmatrix}, \tag{6.17}$$

so that eqs. (6.15) and (6.16) remain valid but

$$\theta^{e,\nu}_{23} \approx 1\,, \qquad \theta^{e,\nu}_{13} \approx \eta' \varepsilon\,, \qquad \theta^{e}_{12} \approx \varepsilon' \tag{6.18}$$

and, most importantly

$$\theta^{\nu}_{12} \approx \eta'/\varepsilon'\,, \tag{6.19}$$

which can make θ_{12} small.

7. Conclusions

The solar and atmospheric neutrino anomalies, strengthened by the recent SuperKamiokande observations, can be interpreted as due to oscillations of the three known neutrinos. However there is still considerable allowed ranges of masses and mixing angles that can account for all these anomalies, especially if a cautious attitude is taken with regard to the theoretical analysis and/or the (difficult) experiments relevant to solar neutrinos. A further major element of uncertainty is related to the relatively large range of values for the mass splitting that can account for the atmospheric neutrino anomaly. We summarize our conclusions by considering a set of alternative hypotheses, related to these dominant uncertainties, with an eye to the experimental program that may lead to their resolution and eventually to the determination of the full set of neutrino oscillation parameters.

A critical value for Δm^2_{23} is around $2 \cdot 10^{-3}\,\mathrm{eV}^2$ mainly because for larger values CHOOZ sets a considerable constraint on the mixing pattern, but also because $(1 \div 2) \cdot 10^{-3}\,\mathrm{eV}^2$ is frequently discussed as a typical sensitivity limit for various Long-Base-Line (LBL) neutrino experiments, like the one from KEK to SK, or the ν_τ appearance experiments with a high energy beam from CERN to Gran Sasso or from Fermilab to Soudan. On the other end, a value of $\Delta m^2_{12} < 2 \cdot 10^{-4}\,\mathrm{eV}^2$, as

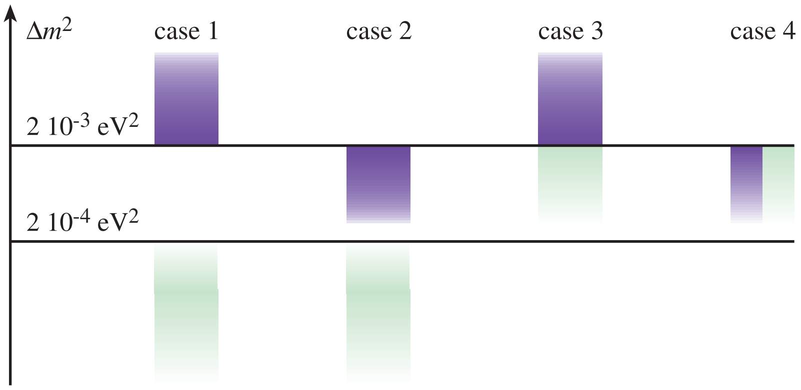

Figure 7: Different combinations of ranges for Δm^2_{23} (dark gray) and Δm^2_{12} (light gray) discussed in the text.

certainly required by a standard Solar Neutrino Analysis (SNA), would make the corresponding oscillation frequency irrelevant to the SK experiment on atmospheric neutrinos. On this basis we consider the following four possibilities, none of which, we believe, can be firmly excluded at present. They are graphically represented in fig. 7.

1. $\Delta m^2_{23} > 2 \cdot 10^{-3}\,\mathrm{eV}^2$ and $\Delta m^2_{12} < 2 \cdot 10^{-4}\,\mathrm{eV}^2$. Here a minimal scheme to describe both solar and atmospheric neutrinos is required, as discussed in section 3, with $\Delta m^2_{23} \gg \Delta m^2_{12}$. Since Δm^2_{12} is too small to affect atmospheric and/or LBL experiments, in both cases eqs. (3.3) – (3.8) apply. The fit relevant to SK is given in fig. 6a, with the further constraint, from CHOOZ, that θ_{13} is small, $\theta_{13} \leq 13°$, and therefore $\theta_{23} = 45° \pm 15°$. In turn θ_{12}, together with Δm^2_{12}, will have to be determined by solar neutrino experiments. In this alternative, the neatest confirmation of the SK result would come from a ν_τ appearance LBL experiment. At the same time, a dominant $\nu_\mu \to \nu_\tau$ oscillation should also lead to a signal in the KEK to SK ν_μ disappearance experiment, with no appreciable ν_e appearance signal.

2. $\Delta m^2_{23} < 2 \cdot 10^{-3}\,\mathrm{eV}^2$ and $\Delta m^2_{12} < 2 \cdot 10^{-4}\,\mathrm{eV}^2$. The main difference with respect to the previous case is that now θ_{13} is not constrained by CHOOZ, and therefore, from fig. 6a, it can be as large as 45°. This implies, from eqs. (3.3) – (3.8), that the results of both atmospheric and LBL experiments, with low enough ν_μ energies to permit exploration of Δm^2 lower than $2 \cdot 10^{-3}\,\mathrm{eV}^2$, may be affected by a significant $P_{\mu e} \neq 0$. By the same token, an experiment with low energy $\bar{\nu}_e$ extending the sensitivity of CHOOZ (e.g. Kam-LAND) may show a large signal if θ_{13} is indeed large. In any event $P_{\mu\tau}$ will be significant. Finally, as in case 1., decoupling of solar and atmospheric neutrino oscillations implies that θ_{12} can only be determined by solar neutrino experiments, with an analysis complicated by θ_{13} being potentially unconstrained (see figs. 3, upper row).

3. $\Delta m^2_{23} > 2\cdot 10^{-3}\,\mathrm{eV}^2$ and $\Delta m^2_{12} > 2\cdot 10^{-4}\,\mathrm{eV}^2$. This case is possible only if SSM constraints are relaxed (fig. 3, lower row) and/or if one of the experimental techniques for solar neutrinos is problematic (fig. 5). However, as discussed in section 4, Δm^2_{12} must be lower than $2\cdot 10^{-3}\,\mathrm{eV}^2$, below the CHOOZ range. Since, on the other hand, $\Delta m^2_{\mathrm{atm}} = \Delta m^2_{23}$ is in the CHOOZ range, θ_{13} is small and eqs. (4.4) – (4.9) are relevant for atmospheric and LBL experiments. The fit of the present SK results gives $\theta_{23} = 45^\circ \pm 25^\circ$ (the range at $\theta_{23} \approx 135^\circ$ being equivalent since θ_{13} is small). Therefore the main difference with respect to case 1. is the possibility of a S_{12} contribution in eqs. (4.4) – (4.9). While ν_τ appearance in LBL experiments must still give a positive signal, $P_{\mu e}$ could significantly deviate from zero at low enough oscillation frequencies (relevant to lower energy ν_μ LBL experiments or to reactor experiments such as Kam-LAND). The finding of such an effect, together with a positive ν_τ appearance signal, would prove, in the three neutrino oscillation picture, the inadequacy of the NSA as it is done now.

4. $\Delta m^2_{23} < 2\cdot 10^{-3}\,\mathrm{eV}^2$ and $\Delta m^2_{12} > 2\cdot 10^{-4}\,\mathrm{eV}^2$. This is the relatively less constrained case (and also the relatively less likely). Here both neutrino squared mass differences are outside of the CHOOZ range, so that θ_{13} is unconstrained. Appropriate values of the mixing angles can fit the SuperKamiokande up/down ratios of atmospheric neutrinos, as shown in fig. 6b. In this case, the two comparable Δm^2 might lead to sizeable CP-violating effects if all the three mixing angles are large.

Measurements by SNO and Borexino will increase the number of independent observational signals of the solar fluxes, S_i, from 3 to 5; so that, from (2.12) with $\Phi_{\mathrm{CNO}}/\Phi_{^7\mathrm{Be}} = 0.22$, $\Delta m^2_{12}, \theta_{12}, \theta_{13}, \Phi_{^7\mathrm{Be}}$ and $\Phi_{^8\mathrm{B}}$ can all be determined. This will provide a crucial consistency check between the experimental techniques and the solar models. If θ_{13} is found to be large, $\Delta m^2_{23} < 2\times 10^{-3}\,\mathrm{eV}^2$, giving a signal at Kam-LAND, but making it harder for LBL experiments.

In the minimal scheme, with a hierarchy amongst the Δm^2, several years of data from Super-Kamiokande will allow a fit to $\Delta m^2_{23}, \theta_{23}$ and θ_{13}. Combining with fits to the solar flux measurements, and to LBL and Kam-LAND experiments, could allow the emergence of a consistent picture for the two oscillation frequencies and the three leptonic mixing angles.

The variety of possibilities discussed above makes it uncertain which is the relevant neutrino mass matrix and, a fortiori, which are the flavour symmetries that might be responsible for it. Nevertheless, focusing on the minimal scheme for both solar and atmospheric neutrinos, the peculiar pattern of masses and mixings renders meaningful the search for an appropriate mass matrix. As discussed in section 5 on general grounds, two forms of mass matrices emerge as being able to describe the data, eqs. (6.1) and (6.2). Since in the minimal scheme $\Delta m^2_{12} \ll 2 \cdot 10^{-3}\,\mathrm{eV}^2$, these forms imply that neutrino masses will not give rise to an observable neutrinoless double beta decay signal. The combination $L_e - L_\mu - L_\tau$ of the individual lepton numbers may play a role in yielding both these forms. A common feature of the resulting solutions is that the heaviest neutrino mass is determined by the oscillation length of the atmospheric neutrinos, $(\Delta m^2_{\rm atm})^{1/2}$. As such, the neutrino masses are irrelevant for present cosmology. Again quite in general, an increasing separation between the two Δm^2 requires the angle θ_{13} to become increasingly small.

Acknowledgments

We thank Zurab Berezhiani for a useful comment. This work was supported in part by the U.S. Department of Energy under Contracts DE-AC03-76SF00098, in part by the National Science Foundation under grant PHY-95-14797, in part by the TMR network under the EEC contract n. ERBFMRX-CT960090.

References

[1] Y. Fukuda et al. (Super-Kamiokande collaboration), *Phys. Rev. Lett.* **81** (1998) 1158 [hep-ex/9805021]; *Erratum Phys. Rev. Lett.* **81** (1998) 4279;
Y. Suzuki (Super-Kamiokande collaboration), in *Neutrino 98, proceedings of the 18th international conference on neutrino physics and astrophysics*, Takayama, Japan, Y. Suzuki and Y. Totsuka eds., to appear on *Nucl. Phys. B (Proc. Suppl.)*.

[2] J.N. Bahcall and M.H. Pinsonneault, *Rev. Mod. Phys.* **67** (1995) 781 [hep-ph/9505425] (BP95);
The recent revision of these fluxes, J.N. Bahcall, S. Basu and M.H. Pinsonneault, *Phys. Lett.* **B 433** (1998) 1 [astro-ph/9805135] (BP98) would not change any of our conclusions.

[3] Y. Fukuda et al. (Super-Kamiokande collaboration), *Phys. Lett.* **B 436** (1998) 33 [hep-ex/9805006].

[4] L. Wolfenstein, *Phys. Rev.* **D 17** (1978) 2369;
S.P. Mikheyev and A. Yu Smirnov, *Sov. J. Nucl. Phys.* **42** (1986) 913.

[5] S.P. Mikheyev and A. Yu Smirnov, *Phys. Lett.* **B 200** (1988) 560;
G. Fogli, E. Lisi and D. Montanino, *Phys. Rev.* **D 54** (1996) 2048 [hep-ph/9605273];
S. Bilenky, C. Giunti and C. Kim *Astrop. Phys.* **4** (1996) 241 [hep-ph/9505301];
T. Teshima, T. Sakai and O. Inagaki, hep-ph/9801276.

[6] S. Parke, *Phys. Rev. Lett.* **57** (1986) 1275;
T.K. Kuo and J. Pantaleone, *Phys. Rev.* **D 35** (1987) 3432.

[7] J.N. Bahcall, *Neutrino astrophysics*, Cambridge University Press 1989.

[8] Solar neutrino fluxes and cross sections can be obtained from the J.N. Bahcall internet page, at www.sns.ias.edu/˜jnb.

[9] For a review and references see V. Castellani et al., *Phys. Rep.* **281** (1997) 309 [astro-ph/9606180].

[10] B.T. Cleveland, *Nucl. Phys.* **38** *(Proc. Suppl.)* (1995) 47;
K. Lande et al., in *Neutrino '96, proceedings of the 17th international con- ference on neutrino physics and astrophysics, Helsinki 1996*, K. Huitu, K. Enqvist and J. Maalampi eds., World Scientific, Singapore 1997.

[11] W. Hampel et al. (Gallex collaboration), *Phys. Lett.* **B 388** (1996) 384;
Gallex Collaboration, TAUP97, Laboratori Nazionali del Gran Sasso September 1997, to appear on Nucl. Phys. B (Proc. Suppl.);
V. Gavrin et al. (SAGE collaboration), *Phys. Lett.* **B 328** (1994) 234; SAGE Collaboration, *Neutrino 96, Helsinki June 1996* to appear on Nucl. Phys. B (Proc. Suppl.).

[12] Y. Fukuda et al., *Phys. Rev. Lett.* **77** (1996) 1683.

[13] N. Hata and P. Langacker, *Phys. Rev.* **D 52** (1995) 420 [hep-ph/9409372]; *Phys. Rev.* **D 56** (1997) 6107 [hep-ph/9705339].

[14] P.I. Krastev and S.T. Petcov, *Phys. Lett.* **B 395** (1997) 69 [hep-ph/9612243].

[15] G.L. Fogli, E. Lisi and D. Montanino, *Astrop. Phys.* **9** (1998) 119 [hep-ph/9709473].

[16] Q.Y. Liu, M. Maris and S. Petcov, *Phys. Rev.* **D 56** (1997) 5991 [hep-ph/9702361];
M. Maris and S. Petcov, *Phys. Rev.* **D 56** (1997) 7444 [hep-ph/9705392].

[17] P. Lipari and M. Lusignuoli, *Phys. Rev.* **D 58** (1998) 073005 [hep-ph/9803440].

[18] M. Honda, T. Kajita, K. Kasahara and S. Midorikawa, *Phys. Rev.* **D 52** (1995) 4985 [hep-ph/9503439].

[19] M. Apollonio et. al (CHOOZ collaboration), *Phys. Lett.* **B 420** (1998) 397 [hep-ex/9711002].

[20] V. Barger, T.J. Weiler, K. Whisnant, *Phys. Lett.* **B 440** (1998) 1 [hep-ph/9807319];
G.L. Fogli, E. Lisi, A. Marrone, G. Scioscia, *Phys. Rev.* **D 59** (1998) 033001 [hep-ph/9808205].

[21] C. Athanassopoulos et al. (LSND collaboration), *Phys. Rev. Lett.* **75** (1995) 2650 [nucl-ex/9504002] ; *Phys. Rev. Lett.* **77** (1996) 3082 [nucl-ex/9706006].

[22] P. Binetruy et al., *Nucl. Phys.* **B 496** (1997) 3 [hep-ph/9610481];
M. Fukugita, M. Tanimoto and T. Yanagida, *Phys. Rev.* **D 57** (1998) 4429 [hep-ph/9709388];
Zhi-zhong Xing, *A phenomenological interpretation of atmospheric and solar neutrino oscillations*, hep-ph/9804433.

[23] M. Drees et al., *Phys. Rev.* **D 57** (1998) 5335 [hep-ph/9712392];
M. Bando, T. Kugo, K. Yoshioka, *Phys. Rev. Lett.* **80** (1998) 3004 [hep-ph/9710417];
V. Barger, S. Pakvasa, T.J. Weiler, K. Whisnant, *Phys. Lett.* **B 437** (1998) 107 [hep-ph/9806387];
S. King, *Phys. Lett.* **B 439** (1998) 350 [hep-ph/9806440].

[24] M. Gell-Mann, P. Ramond, and R. Slansky, in *Supergravity* P. van Nieuwenhuizen and D.Z. Freedman eds., North-Holland, Amsterdam 1979, p. 315;
T. Yanagida, in *Proceedings of the workshop on the unified theory and the baryon number in the universe* O. Sawada and A. Sugamoto eds., KEK Report No. 79-18, Tsukuba, Japan 1979.